Loebermann, H., Tokuoka, R., Deisenhofer, J., & Huber, R. (1984) *J. Mol. Biol. 177*, 531–556.
McGrogan, M., Kennedy, J., Ping Li, M., Hsu, C., Scott, R. W., Simonsen, C. C., & Baker, J. B. (1988) *Bio/Technology 6*, 172–177.
Monard, D., Solomon, F., Rentsch, M., & Gysin, R. (1973) *Proc. Natl. Acad. Sci. U.S.A. 70*, 1894–1897.
Monard, D., Niday, E., Limat, A., & Solomon, F. (1983) *Prog. Brain Res. 58*, 359–363.
Reinhard, E., Meier, R., Halfter, W., Rovelli, G., & Monard, D. (1988) *Neuron 1*, 387–394.
Schürch-Rathgeb, Y., & Monard, D. (1978) *Nature 273*, 308–309.
Scott, R. W., Bergmann, B. L., Bajpai, A., Hersh, R. T., Rodriguez, H., Jones, B. N., Barreda, C., Watts, S., & Baker, J. B. (1985) *J. Biol. Chem. 260*, 7029–7034.
Smith, C. E., & Johnson, D. A. (1985) *Biochem. J. 225*, 463–472.
Sommer, J., Gloor, S., Rovelli, G. F., Hofsteenge, J., Nick, H., Meier, R., & Monard, D. (1987) *Biochemistry 26*, 6407–6410.
Stone, S., Nick, H., Hofsteenge, J., & Monard, D. (1987) *Arch. Biochem. Biophys. 252*, 237–244.
Towbin, H., Staehelin, T., & Gordon, J. (1979) *Proc. Natl. Acad. Sci. U.S.A. 76*, 4350–4354.
Walker, C., Wilkstrom, C., & Shaw, E. (1985) *Biochem. J. 230*, 645–650.
Zurn, A. D., Nick, H., & Monard, D. (1988) *Dev. Neurosci. 10*, 17–24.

Allosteric Effects Acting over a Distance of 20–25 Å in the *Escherichia coli* Tryptophan Synthase Bienzyme Complex Increase Ligand Affinity and Cause Redistribution of Covalent Intermediates†

Karl F. Houben‡ and Michael F. Dunn*
Department of Biochemistry, University of California at Riverside, Riverside, California 92521
Received June 26, 1989; Revised Manuscript Received October 26, 1989

ABSTRACT: The reactions of L-histidine (L-His) and L-tryptophan (L-Trp) with the $\alpha_2\beta_2$ complex of *Escherichia coli* tryptophan synthase are introduced as probes both of β-subunit catalysis and of ligand-mediated α–β allosteric interactions. Binding of DL-α-glycerol 3-phosphate (GP), an analogue of 3-indole-D-glycerol 3′-phosphate (IGP), to the α-catalytic site increases the affinity of $\alpha_2\beta_2$ for L-His 4.5-fold and the affinity for L-Trp 17-fold and brings about a redistribution of β-bound intermediates that favors the quinonoids derived from each amino acid. Inorganic phosphate (P_i) (presumably via binding to the α-catalytic site) influences the distribution of L-His intermediates as does GP. Previous binding studies [Heyn, M. P., & Weischet, W. O. (1975) *Biochemistry 14*, 2962–2968] indicate that when the phosphoryl group subsite of the α-catalytic site is occupied by GP or P_i, a high-affinity indole subsite is induced at the α-catalytic site. Interaction of benzimidazole (BZ), an analogue of indole, with this site also shifts the distribution of β-bound L-His intermediates in favor of the L-His quinonoid. In the absence of P_i or GP, BZ interacts primarily at the β-catalytic site and competes with L-His for the β-subunit indole subsite. Since L-His and GP (or P_i) are substrate analogues and L-Trp is the physiological product, these allosteric effects likely take place with the natural substrates. Accordingly, the β-site becomes a higher affinity site for L-Ser, and L-Ser is in a more chemically reactive form when IGP (or D-glyceraldehyde 3-phosphate) is bound at the α-catalytic site. Hence, we postulate that, in vivo, ligand binding at the α-catalytic site confers changes to the β-catalytic site which increase the probability of L-Trp formation via an increased likelihood of L-Ser condensation with indole.

In biological systems, the control of protein function via allosteric regulation involves binding interactions at loci on the protein surface which bring about a change in conformation and a consequent change in properties at other loci. Most hypotheses to explain the behavior of allosteric protein systems have been restricted to models concerned with the modulation of ligand affinity via the binding of homotropic and heterotropic effectors (Monod et al., 1965; Koshland et al., 1966). In this paper, we introduce evidence indicating that long-range heterotropic binding can also alter the chemical reactivities and thermodynamic stabilities of covalent intermediates.

Native tryptophan synthase from *Escherichia coli* (EC 4.2.1.20) is a bienzyme complex with subunit composition $\alpha_2\beta_2$ that catalyzes the last two steps in the biosynthesis of L-tryptophan (L-Trp)[1] (Kirschner et al., 1975a; Miles, 1979).

†This work was supported by NSF Grants DMB-84-08513 and DMB-87-03697.
*Address correspondence to this author at the Department of Biochemistry, University of California at Riverside, Riverside, CA 92521-0129.
‡Present address: Department of Biological Chemistry, University of California, Los Angeles, CA 90024-4280.

[1] Abbreviations: PLP, pyridoxal 5′-phosphate; L-His, L-histidine; L-Ser, L-serine; L-Trp, L-tryptophan; $\alpha_2\beta_2$, the native form of *E. coli* tryptophan synthase (EC 4.2.1.20); E(Ain-E) and E(Ain-K), internal ϵ-aminolysyl aldimine enolimine and ketoenamine tautomers, respectively, of enzyme-bound PLP; E(S), enzyme–L-His or –L-Trp Michaelis complexes; E(GD), geminal diamine intermediate formed in the reaction of either L-Trp or L-His with the internal aldimine form of enzyme-bound PLP; E(Aex-K) and E(Aex-E), external aldimine ketoenamine and enolimine tautomers, respectively, formed with L-Trp or L-His; E(Q), quinonoid intermediate; GP, DL-α-glycerol 3-phosphate; IGP, 3-indole-D-glycerol 3′-phosphate; BZ, benzimidazole; P_i, inorganic phosphate; G3P, D-glyceraldehyde 3-phosphate; AU, absorbance unit(s).

0006-2960/90/0429-2421$02.50/0

Scheme I: Organic Structures Showing the Expected Tautomeric States and Ionization States and Positions of UV–Visible Absorption Bands for the Species Formed in the Reactions of L-His and L-Trp with PLP Bound to the β-Subunits of Tryptophan Synthase

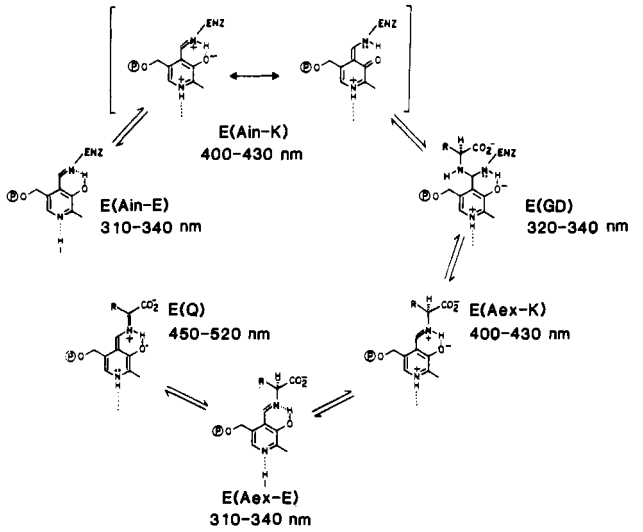

The overall reaction, eq 1, is catalyzed by the native $\alpha_2\beta_2$ enzyme. The α and β_2 components can be separated and isolated (Yanofsky & Crawford, 1972; Miles, 1979). The α-subunit catalyzes a reverse aldol condensation-like reaction in which 3-indole-D-glycerol 3′-phosphate (IGP) is converted to indole and D-glyceraldehyde 3-phosphate (G3P) (eq 2).

$$\text{IGP} + \text{L-Ser} \xrightarrow{\alpha_2\beta_2} \text{L-Trp} + \text{G3P} + \text{H}_2\text{O} \quad (1)$$

$$\text{IGP} \xrightleftharpoons{\alpha \text{ or } \alpha_2\beta_2} \text{indole} + \text{G3P} \quad (2)$$

$$\text{indole} + \text{L-Ser} \xrightarrow{\beta_2 \text{ or } \alpha_2\beta_2} \text{L-Trp} + \text{H}_2\text{O} \quad (3)$$

The pyridoxal phosphate (PLP) requiring β-subunits catalyze the condensation of L-serine (L-Ser) and indole to form L-Trp (eq 3). The rates of the reactions described by eqs 2 and 3 are greatly increased (approximately 100- and 50-fold, respectively) when catalyzed by the $\alpha_2\beta_2$ oligomer (Yanofsky & Crawford, 1972).

The X-ray structure of $\alpha_2\beta_2$ tryptophan synthase from *Salmonella typhimurium* has been solved to 2.5-Å resolution (Hyde et al., 1988). Because the *S. typhimurium* and *E. coli* enzymes exhibit highly homologous amino acid sequences, the three-dimensional structures of the two must be almost identical. Earlier studies of *E. coli* tryptophan synthase using other methods indicated the $\alpha_2\beta_2$ complex has an almost linear α–β–β–α arrangement (Wilhelm et al., 1982) and the distance between active sites of the α- and β-subunits is 20–25 Å (Lane & Kirschner, 1983). The X-ray structure of *S. typhimurium* $\alpha_2\beta_2$ has established the linear arrangement of subunits. The structure shows there are α–β and β–β subunit interfaces, but no α–α interfaces. One of the most significant results of the X-ray crystallography studies is the identification of a 20–25-Å long hydrophobic tunnel connecting the α- and β-catalytic sites. The existence of this tunnel is consistent with a channeling mechanism (Srivastava & Bernhard, 1986a,b) for the transfer of indole from the α-site to the β-site [as proposed by Matchett (1974) for tryptophan synthase of *Neurospora crassa*]. Additionally, the tunnel explains the absence of free indole in eq 1. A recent study has proposed and presented evidence that the channeling of indole between α- and β-sites is the highly preferred mechanism of transfer (Dunn et al., 1987).

Investigations of the reactions of the L-Ser analogues L-histidine (L-His) and L-Trp have shown that $\alpha_2\beta_2$ yields

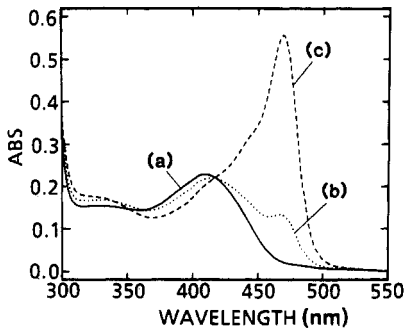

FIGURE 1: Spectra of (a) 39 μN $\alpha_2\beta_2$, (b) 39 μN $\alpha_2\beta_2$ and 200 mM L-His, (c) 39 μN $\alpha_2\beta_2$, 200 mM L-histidine, and 25 mM GP in 0.05 M Bicine buffer and 1 mM EDTA, pH = 7.8, 25 °C.

equilibrating mixtures of external aldimine [E(Aex-K) and E(Aex-E)], quinonoid species E(Q), and possibly other intermediates shown in Scheme I (Kirschner et al., 1975b; Lane & Kirschner, 1981; Kawasaki et al., 1987; Houben et al., 1989; Drewe et al., 1989). Herein, we investigate the influence of allosteric effectors on the reactions of L-His and L-Trp with the $\alpha_2\beta_2$ complex via equilibrium binding, and rapid kinetic studies of the L-His reaction are also presented. As will be shown, the binding of DL-α-glycerol 3-phosphate (GP), or phosphate ion (P_i), to the α-subunit, catalytic site brings about a redistribution of bound covalent intermediates 25 Å away at the β-catalytic site and increases the affinity of the β-site for substrate and/or analogue. The allosteric effects of benzimidazole (BZ), an indole analogue, are also investigated.

Materials and Methods

All analogue molecules used were purchased from Sigma (reagent grade). Purification of tryptophan synthase from *E. coli* has been described (Adachi et al., 1974; Miles & Moriguchi, 1977; Tschopp & Kirschner, 1980; Drewe & Dunn, 1985). Spectroscopic measurements were carried out as described by Houben et al. (1989). All of the titrations reported herein were measured by following the absorbance changes at 468 nm.

Rapid-Scanning Stopped-Flow (RSSF) Spectrometry. The RSSF instrumentation used in this study is identical with that used in a previous study (Houben et al., 1989). For the spectra in Figure 3, the collection of the first scan relative to flow cessation is noted in the figure legends. The repetitive scan rate is 8.9 ms. The second through tenth scans in Figure 3A were collected at the following intervals after the first: (2) 8.9, (3) 17.8, (4) 26.7, (5) 35.6, (6) 44.5, (7) 53.4, (8) 62.3, (9) 80.1, (10) 97.9, (11) 133.5, (12) 160.2, (13) 195.8, and (14) 240.3 ms. The second through fourteenth scans in Figure 3B were collected at the following intervals after the first: (2) 8.9, (3) 17.8, (4) 26.7, (5) 35.6, (6) 44.5, (7) 53.4, (8) 62.3, (9) 71.2, (10) 80.1, (11) 89.0, (12) 106.8, (13) 124.6, and (14) 160.2 ms.

Results

Reaction of the $\alpha_2\beta_2$ complex of tryptophan synthase with L-His gives new UV–visible spectral bands (Figure 1, spectrum b) that previously have been assigned to the external aldimine E(Aex_1) ($\lambda_{max} \simeq 413$ nm) and to the quinonoid E(Q) ($\lambda_{max} \simeq 468$ nm, see Scheme I)(Houben et al., 1989). When GP is bound, the amplitudes of the bands attributed to the quinonoid structure increase, while the band attributed to the external aldimine decreases (Figure 1, spectrum c).

L-His Titration Studies. The dependences of the spectral changes shown in Figure 1 on the concentration of L-His are conveniently measured by monitoring the increase in absor-

Table I: Summary of Rate and Equilibrium Data for the Effects of DL-Glycerol 3-Phosphate and Phosphate Ions on the Reaction of L-Histidine with *E. coli* Tryptophan Synthase

relaxation kinetic studies[a]					equilibrium binding studies[d]		
reactant and preincubation conditions		apparent rate constant[b] (s^{-2})					
syringe 1	syringe 2	$1/\tau$	$1/\tau_1$	$1/\tau_2$	concentrations	ligand varied	apparent dissociation constant
$[\alpha_2\beta_2]$ = 80 μN	[L-His] = 5–30 μM [L-His] = 30 μM–50 mM	20 ± 5	37 ± 10	16 ± 7	$[\alpha_2\beta_2]$ = 18 μN	L-His	$K_{\text{L-His}}$ = 22 mM
$[\alpha_2\beta_2]$ = 47 μN, [GP] = 40 mM	[L-His] = 0.15–5 mM [L-His] ≥ 50 mM	20 ± 5	43 ± 10	15 ± 2	$[\alpha_2\beta_2]$ = 18 μN, [GP] = 50 mM	L-His	$K^{\text{GP}}_{\text{L-His}}$ = 4.8 mM
$[\alpha_2\beta_2]$ = 18 μN, [L-His] = 189 mM	[GP] = 1.0–45 mM		62 ± 10	20 ± 5	$[\alpha_2\beta_2]$ = 28 μN, [L-His] = 180 mM	GP	$K^{\text{L-His}}_{\text{GP}}$ = 0.4 mM
$[\alpha_2\beta_2]$ = 18 μN, [L-His] = 189 mM	[P_i] = 67–108 mM_{em}[c]		18 ± 5	7 ± 3	$[\alpha_2\beta_2]$ = 28 μN, [L-His] = 140 mM	P_i	$K^{\text{L-His}}_{\text{em}}$ = 46 mM_{em}[c]
$[\alpha_2\beta_2]$ = 18 μN, [L-His] = 189 mM	[GP] = 20 mM, [P_i] = 67 mM_{em}[c]		28 ± 7	8 ± 4	$[\alpha_2\beta_2]$ = 24 μN, [L-His] = 87 mM, [GP] = 24 mM	P_i	$K^{\text{L-His,GP}}_{\text{em}}$ = 136 mM_{em}[c]

[a] Measured in 0.05 M Bicine buffer, pH 7.8, and 1 mM EDTA at 25 °C. Components preincubated before mixing in the stopped-flow apparatus are listed under syringe 1 or syringe 2, respectively. Concentrations refer to conditions immediately *after* mixing the contents of syringes 1 and 2 in the stopped flow. $\alpha_2\beta_2$ concentrations refer to the normality of β-sites. Measured equilibrium constants are assumed to be determined with an accuracy ~±25%. [b] Analysis according to eq 5; see text. [c] Phosphate ion concentrations and equilibrium constants are given in units of effective mass. [d] Binding titration data were fit to the hyperbolic (Langmuir) isotherm; see eq 4, text.

bance at 468 nm. When these experiments are carried out in 0.1 M potassium phosphate buffer and 1 mM EDTA at pH 7.80 (the typical working medium for tryptophan synthase), the titration data do not satisfactorily fit a single hyperbolic equation (data not shown). When the 0.1 M potassium phosphate buffer is replaced by 0.05 M Bicine buffer while keeping all other conditions constant, titration of the $\alpha_2\beta_2$ complex with L-His produces data (Figure 2A) that are well described by a single hyperbolic (Langmuir) isotherm:

$$\Delta A = \Delta A_{max}[S]/\{[S] + K\} \quad (4)$$

where ΔA is the change in absorbance, ΔA_{max} is the maximum change in absorbance at infinite substrate concentration, [S] is the concentration of free substrate, and K is the concentration of free substrate at $^1/_2\Delta A_{max}$. K values for titrations carried out under various conditions are summarized in Table I. Assuming identical and independent sites and a β-site:L-His stoichiometry of 1:1, computer best fits give $K_{\text{L-His}}$ = 22 mM when the $\alpha_2\beta_2$ complex is titrated with L-His in 0.05 M Bicine buffer (Figure 2A, isotherm a, and Table I). The UV–visible spectral properties of the $\alpha_2\beta_2$–L-His system are insensitive to changes in the concentration of Bicine buffer. Since, at saturating L-His concentrations, the exclusion of phosphate ion (P_i) also decreases the amplitude of the 468-nm band, it was concluded that the role played by P_i in this system should be further delineated. Titration of the $\alpha_2\beta_2$(L-His)$_2$ complex with P_i gives data (Figure 2B, isotherm b) that, when corrected for phosphate activity, yield a $K^{\text{L-His}}_{\text{em}}$ value of 46 mM_{em} (in effective mass units). The low values of the P_i activity coefficient at the concentrations of P_i used make it necessary to express the chemical potential of P_i as effective mass (Robinson & Stokes, 1968). When the $\alpha_2\beta_2$ complex is preequilibrated with saturating GP in Bicine buffer, titration with L-His gives a best-fit value of $K^{\text{GP}}_{\text{L-His}}$ = 4.8 mM (Figure 2A, isotherm b, and eq 4). When the $\alpha_2\beta_2$ complex preequilibrated with L-His is titrated with GP (Figure 2B, isotherm a), computer best-fit values to eq 4 give $K^{\text{L-His}}_{\text{GP}}$ = 0.4 mM (assuming only the D-isomer of GP binds to the enzyme). Because P_i at pH 7.8 has a $K^{\text{L-His}}_{\text{em}}$ value of 46 mM_{em} and because the activity coefficient of P_i is highly concentration-dependent, it is very difficult to saturate the system with P_i. For example, a 1.0 M solution of potassium phosphate corresponds to a solution of approximately 231 mM_{em}, a value that gives only 83% of the extrapolated ΔA_{max} of the Langmuir isotherm (eq 4). Hence, all rapid kinetic experiments reported herein (except those to specifically investigate the P_i effect) were performed in solutions buffered with 0.05 M Bicine instead of 0.1 M potassium phosphate.

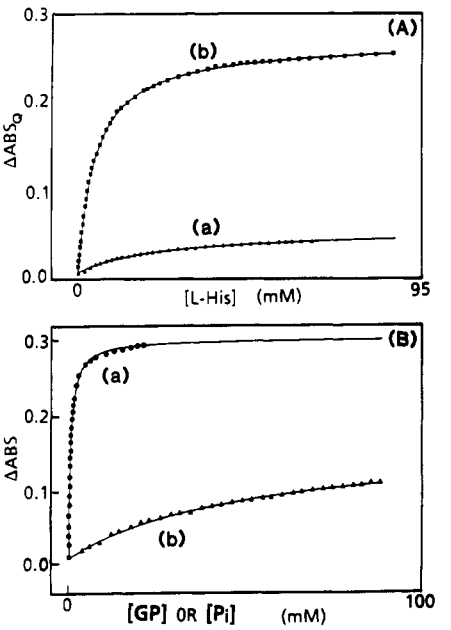

FIGURE 2: Titration data measured at 468 nm. (A) Addition of (a) L-His to 18 μN $\alpha_2\beta_2$ and (b) L-His to 18 μN $\alpha_2\beta_2$ and 50 mM GP. (B) Addition of (a) GP to 28 μN $\alpha_2\beta_2$ and 180 mM L-His and (b) P_i to 28 μN $\alpha_2\beta_2$ and 140 mM L-His. Other conditions were similar to those in Figure 1. The best-fit K values (assuming eq 4 applies) are (A) (a) 22 mM, (b) 4.8 mM, and (B) (a) 0.4 mM, (b) 47 mM (in effective mass units).

Rapid-Scanning Stopped-Flow (RSSF) Spectroscopic Studies. Figure 3 shows the results obtained in RSSF UV–visible spectroscopic experiments both when L-His is mixed with the $\alpha_2\beta_2$ complex in the absence of GP (Figure 3A) and

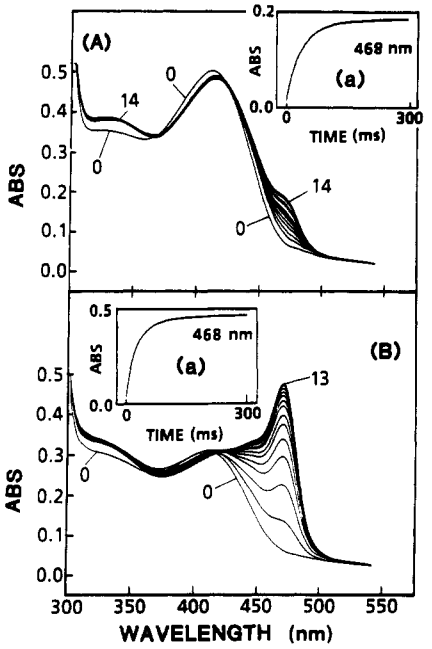

FIGURE 3: Rapid-scanning stopped-flow spectra showing the spectral changes for the reactions of (A) the $\alpha_2\beta_2$ enzyme with L-His and (B) the $\alpha_2\beta_2$ enzyme preequilibrated in GP with L-His. Before mixing, in (A) the enzyme was contained in one syringe while L-His was contained in the other syringe, and in (B) the enzyme and GP were contained in one syringe while L-His was contained in the other syringe. The insets are the single-wavelength time courses at 468 nm. The initiation of scanning in (A) and (B) occurred 1 and 3 ms, respectively, after flow stopped. The traces designated 0 are the reconstructed spectra of the reactants. See Materials and Methods for the timing sequence. Conditions after mixing: (A) 80 μN $\alpha_2\beta_2$ and 134 mM L-His; (B) 47 μN $\alpha_2\beta_2$, 134 mM L-His, and 40 mM GP. In each experiment the buffer was 0.05 M Bicine, 1 mM EDTA, pH 7.80, 25 °C. Assuming a biphasic time course, the best fits of the data shown in insets are as follows: (A) $A_1 = 0.09$, $1/\tau_1 = 36$ s^{-1}, and $A_2 = 0.08$, $1/\tau_2 = 17$ s^{-1}; (B) $A_1 = 0.33$, $1/\tau_1 = 50$ s^{-1}, and $A_2 = 0.09$, $1/\tau_2 = 15$ s^{-1}.

when $\alpha_2\beta_2$ has been preequilibrated with GP (Figure 3B). The family of time-resolved spectra (Figure 3A) for the wavelength range 300–550 nm shows that a band with $\lambda_{max} \simeq 468$ nm is formed while the 410-nm band decreases and the band at 335 nm increases in amplitude. The changes in the amplitudes of these bands are enhanced when L-His is mixed with $\alpha_2\beta_2$ preincubated with GP (Figure 3B) or P_i (data not shown).

The time courses of the spectral changes shown in Figure 3 are biphasic, and the changes at 335, 410, and 468 nm appear to be due to concomitant processes. During the slower phase (Figure 3B), there is an isoabsorption point[2] at approximately 422 nm for the reaction of L-His with $\alpha_2\beta_2$ preincubated with GP.

Single-Wavelength Stopped-Flow Studies. Single-wavelength stopped-flow (SWSF) studies of the reaction of L-His with $\alpha_2\beta_2$, and with $\alpha_2\beta_2$ preincubated either with GP or with P_i, or when $\alpha_2\beta_2$ is preincubated with L-His and then mixed with GP or P_i, were performed by monitoring the changes in absorbance at 468 nm. The reaction of L-His with $\alpha_2\beta_2$ is characterized by a single relaxation at low L-His concentrations (i.e., 5–30 mM). These time courses are well described by eq 5 for the case where n is equal to 1, where $1/\tau_i$ is the ith

$$A_t = A_\infty \pm \sum_{i=1}^{n} A_i \exp(-t/\tau_i) \qquad (5)$$

[2] The term "isoabsorption point" designates a wavelength where the absorbance remains constant (unchanging) during one or more but not all phases of the reaction.

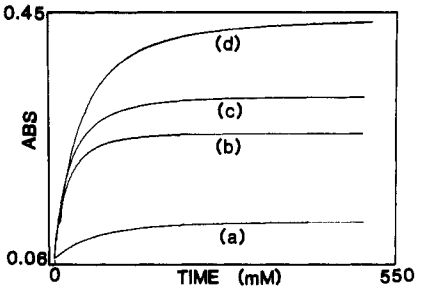

FIGURE 4: Single-wavelength, stopped-flow time courses monitored at 468 nm of the reaction of $\alpha_2\beta_2$ preequilibrated in saturating L-His with GP or P_i. Before mixing, in (a) $\alpha_2\beta_2$ and L-His are contained in one syringe while P_i and L-His are contained in the other, in (b) $\alpha_2\beta_2$ and L-His are contained in one syringe while GP and L-His are contained in the other syringe, and in (d) $\alpha_2\beta_2$ and L-His are contained in one syringe while GP, P_i, and L-His are contained in the other syringe. The concentration of L-His is equivalent in all syringes. Trace c shows the simulated sum of traces a and b. Conditions after mixing are as follows: (a) $[P_i] = 163$ mM, (b) [GP] = 20 mM, (d) $[P_i] = 163$ mM_{em}, and [GP] = 20 mM. In each experiment $[\alpha_2\beta_2] = 18$ μN, [L-His] = 189 mM, and the buffer was 0.05 M Bicine and 1 mM EDTA, pH 7.8, 25 °C. Assuming a biphasic time course, the best fits of the data are as follows: (a) $A_1 = 0.04$, $1/\tau_1 = 18.8$ s^{-1}, and $A_2 = 0.02$, $1/\tau_2 = 7.8$ s^{-1}; (b) $A_1 = 0.13$, $1/\tau_1 = 63$ s^{-1}, and $A_2 = 0.07$, $1/\tau_2 = 20$ s^{-1}; (d) $A_1 = 0.22$, $1/\tau_1 = 31$ s^{-1}, and $A_2 = 0.14$, $1/\tau_2 = 8.5$ s^{-1}.

observed rate constant for the absorbance increase at 468 nm, A_∞, A_i, and A_t are respectively the absorbance at infinite time, the ith amplitude corresponding to $1/\tau_i$, and the absorbance at time t. Kinetic data (rate constants and amplitudes) are summarized in Table I. At higher L-His concentrations (inset, Figure 3A), there are at least two relaxations. These time courses are well described when fit to a sum of two exponentials (eq 5 with $n = 2$); however, because the two processes are not well separated in rate, the exact values of the observed rates cannot be extracted from these data.

When $\alpha_2\beta_2$ is preincubated with GP, the time course of the reaction obtained at low concentrations of L-His (0.15–5.0 mM) also is adequately described by a single exponential expression (eq 5 with n equal to 1). At higher L-His concentrations (≥50 mM), the expression consisting of the sum of two exponentials ($n = 2$, eq 5) provides a better fit (inset, Figure 3B). Preincubation with GP increases the amplitudes of the 468-nm changes.

The absorbance changes measured at 468 nm for the reaction of L-His both with the $\alpha_2\beta_2$ complex and with the $\alpha_2\beta_2$ complex preequilibrated with GP are very similar. Both systems yield apparently identical relaxations at low L-His concentration, and both systems give biphasic time courses at higher L-His concentrations. The detection of two relaxations implies at least three states. The simplest mechanism that is consistent with the data is

$$A + B \underset{k_{-1}}{\overset{k_1}{\rightleftharpoons}} C \underset{k_{-2}}{\overset{k_2}{\rightleftharpoons}} D \qquad (6)$$

The behavior of both systems indicates that these processes are tightly coupled.

Effects of GP, P_i, and BZ on the $\alpha_2\beta_2$–L-His Complex. The SWSF studies of the effects of GP nd P_i on the $\alpha_2\beta_2$ complex preequilibrated with saturating L-His are interesting. When 1.0–45 mM GP is rapidly mixed with the $\alpha_2\beta_2$(L-His)$_2$ complex, the time course of the 468-nm changes (Figure 4, trace b) is well described by the fit to a sum of two exponentials (eq 5) with $1/\tau$ values of 62 ± 10 and 20 ± 5 s^{-1}. When the experiments are repeated but with P_i (163–326 mM or 67–108 mM_{em}) substituted for GP, the time course (Figure 4, trace a) also consists of two exponentials with $1/\tau$ values of 18 ±

5 and 7 ± 3 s^{-1} (Table I). Again, two relaxations imply at least three states. The binding of GP (or P_i) to the α-subunit (i.e., the bimolecular process) is not directly detected. The binding of either GP or P_i almost certainly is rapid relative to the observed relaxations; therefore, it is not surprising that the relaxation rates for both the GP and P_i systems appear to be independent of concentration. Only those induced conformational changes transmitted from the α-site to the β-site that confer spectral changes to the PLP chromophore via redistribution of intermediates are detected. Because the β substrate site (the source of the chromophoric signal) is saturated with L-His, the observed relaxations must be due to at least two, tightly-coupled, true unimolecular processes and are consistent with the mechanism:

$$X \underset{k_{-a}}{\overset{k_a}{\rightleftharpoons}} Y \underset{k_{-b}}{\overset{k_b}{\rightleftharpoons}} Z \qquad (7)$$

Equation 7 has been solved explicitly for the general case; unfortuantely, the determination of intrinsic rate constants of tightly coupled first-order series reactions where none of the initial concentrations are zero is difficult and is nearly impossible in the absence of an accurate knowledge of the concentrations of the components involved (Moore & Pearson, 1981).

The absorbance amplitude obtained when both GP and P_i are mixed with the $\alpha_2\beta_2$ complex preequilibrated with saturating L-His is significantly greater than the sum of the amplitudes obtained with equivalent concentrations of either GP or P_i alone. Twenty millimolar GP (Figure 4, trace b) gives an increase at 468 nm of 0.19 absorbance unit (AU) (at t_∞), while 163 mM_{em} P_i (Figure 4, trace a) gives an increase of 0.06 AU (at t_∞) when mixed with the $\alpha_2\beta_2$ complex preequilibrated with saturating L-His. The sum of these amplitudes (simulated trace c) is 0.25 AU (at t_∞). When both GP (20 mM) and P_i (163 mM_{em}) are rapidly mixed with the same $\alpha_2\beta_2$(L-His)$_2$ complex, the amplitude increase at 468 nm is 0.35 AU (Figure 4, trace d). Hence, GP and P_i act in concert to produce an amplitude change $\simeq$40% greater than the sum of the separate effects of GP and P_i. The time course resulting from the mixing of GP (20 mM) and P_i (163 mM_{em}) with $\alpha_2\beta_2$ preequilibrated with saturating L-His is best fit to a sum of two exponentials (eq 5) with average $1/\tau$ values of 28 ± 7 and 8 ± 4 s^{-1}.

In view of the results of these SWSF studies, a titration experiment involving the addition of P_i to the $\alpha_2\beta_2$ complex preequilibrated with saturating concentrations of GP (24 mM) and L-His (87 mM) was undertaken. The results are shown in Figure 5A and Table I. The concentration dependence is satisfactorily described by the Langmuir isotherm (eq 4) with a best-fit value for $K_{em}^{L\text{-His,GP}}$ of 136 mM_{em}.

Data derived from the titration of the $\alpha_2\beta_2$(L-His)$_2$ complex with BZ (monitored at 468 nm) in the presence (trace a) and absence of P_i (trace b) are shown in Figure 5B. The absorption changes in 0.1 M potassium phosphate (isotherm a) are biphasic, initially increasing and then decreasing. These absorption changes are characteristic of ligand binding at two classes of sites with different affinities for the ligand. Binding at the higher affinity site increases the absorption at 468 nm, while binding at the lower affinity site diminishes the 468-nm absorption. In the absence of P_i (isotherm b), the absorption at 468 nm decreases as BZ is added to the $\alpha_2\beta_2$ complex.

L-Trp Titration Studies. The studies of Lane and Kirschner (1981) show that the intensity of the quinonoid band (λ_{max} 476 nm) formed as L-Trp reacts with $\alpha_2\beta_2$ is enhanced when the IGP analogue 3-indolepropanol 3′-phosphate (IPP) is bound to the α-site. Their studies were carried out in phosphate buffer and, thus, were limited in scope. Herein, we present additional binding studies in Bicine buffer to explore the effects of reciprocal site–site interactions on the binding of L-Trp to the β-sites and GP to the α-sites. It was found that GP causes effects similar to those described in Figures 1–6 and Table I for the L-His–GP system. When the α-sites are saturated with GP, the amplitude of the L-Trp quinonoidal band is increased approximately 4-fold in Bicine buffer without changing the band shape or position. The results of the L-Trp

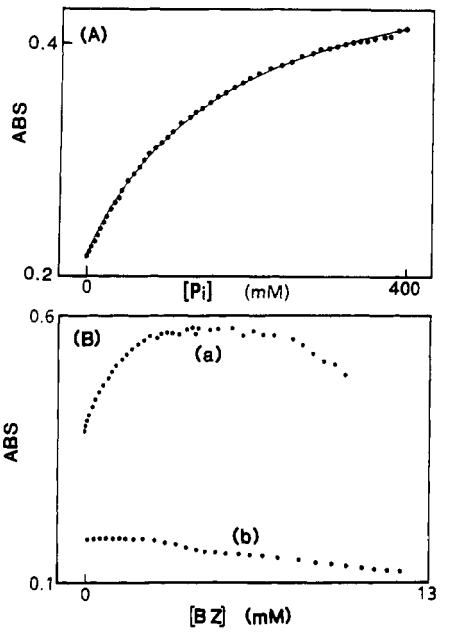

FIGURE 5: (A) Absorption changes at 468 nm on addition of P_i to 16 μN $\alpha_2\beta_2$, 24 mM GP, and 87 mM L-His. Conditions are similar to those in Figure 1. Note that the abscissa is in units of effective mass (see text). The best-fit $K^{L\text{-His,GP}}$ = 136 mM effective mass. (B) Absorption changes at 468 nm on addition of BZ to (a) 79 μN $\alpha_2\beta_2$ and 95 mM L-His in 0.1 M phosphate buffer and (b) 79 μN $\alpha_2\beta_2$ and 75 mM L-His in 0.05 M Bicine buffer. Both experiments were carried out in 1 mM EDTA, pH 7.8, 25 °C.

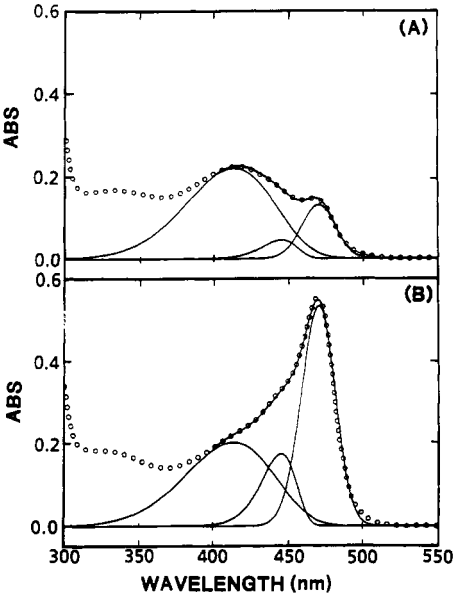

FIGURE 6: Log-normal distribution curve fits covering the absorption region from 400 to 550 nm of (A) the complex formed with $\alpha_2\beta_2$ and L-His and (B) the complex formed with $\alpha_2\beta_2$, L-His, and GP. The conditions are identical with those shown in Figure 1. The solid line through the experimental points (O) is the sum of the log-normal curves which are shown individually below the solid line. The absorption spectra were corrected for base-line errors and small amounts of turbidity as in Likos et al. (1982).

Table II: Summary of Equilibrium Data for the Effects of DL-Glycerol 3-Phosphate on the Reaction of L-Tryptophan with *E. coli* Tryptophan Synthase[a]

concentrations	ligand varied	apparent dissociation constant
$[\alpha_2\beta_2]$ = 26.5 μN	L-Trp	$K_{L\text{-}Trp}$ = 0.35 mM
$[\alpha_2\beta_2]$ = 6.63 μN, [GP] = 50 mM	L-Trp	$K^{GP}_{L\text{-}Trp}$ = 0.020 mM
$[\alpha_2\beta_2]$ = 26.5 μN, [L-Trp] = 10 mM	GP	$K^{L\text{-}Trp}_{GP}$ = 0.46 mM

[a] Conditions are the same as described in Table I and data were analyzed similarly except where concentrations of $\alpha_2\beta_2$ were smaller than values of K. In these instances, analysis involved use of the quadratic form of the binding equation as in Lane and Kirschner (1981). Measured equilibrium constants are assumed to be determined with an accuracy of ±25%.

binding titrations are summarized in Table II. GP binding increases the apparent affinity of the β-sites for L-Trp by about 17-fold. Kinetic data describing the influence of GP on the reaction of $\alpha_2\beta_2$ with L-Trp in Bicine buffer will be presented elsewhere (Dunn et al., in preparation).

Discussion

Binding of DL-*Glycerol 3-Phosphate to the α-Site Induces Redistribution of Covalent Intermediates at the β-Site.* Upon reaction with L-His, the PLP moiety of the $\alpha_2\beta_2$ complex of tryptophan synthase forms UV–visible spectral bands (Figures 1, spectrum b, and 3A) corresponding to chemical intermediates along the catalytic pathway (Houben et al., 1989). Since the absorption bands of many chemical structures have highly characteristic log-normal parameters (Metzler et al., 1980, 1985), the parameters of the log-normal distribution curve provide a means of deconvoluting overlaping spectral structure of absorbing chemical species.[3] Four parameters define a log-normal distribution curve (Siano & Metzler, 1969): the λ_{max} of the curve, the amplitude, the width of the curve at half-height (HW), and the skewness of the curve (Ω). The spectral changes induced by GP binding could be due either to a ligand-induced redistribution of PLP species or to a ligand-induced perturbation of the β-site that alters the microenivronment of the PLP chromophore and thereby perturbs the electronic spectra of the PLP species. If GP binding to the α-subunit causes a redistribution of the L-His intermediates, then it should be possible to fit those absorption bands of both spectra that correspond to these chemical intermediates with log-normal distribution curves by varying only the amplitude parameter (the parameter that defines the concentration of the chemical species involved). However, if the PLP microenvironment is perturbed, then there should be detectable changes in λ_{max}, band width, and skewness.

The analysis presented in Figure 6 and Table III strongly indicates that the PLP absorption spectra of the L-His–$\alpha_2\beta_2$ system both in the presence and in the absence of GP (Figure 6) *represent different distributions of the same chemical intermediates*, not spectra of absorption bands that have been perturbed by environmental factors such as differences in polarity or changed interactions of neighboring groups which alter λ_{max} and/or band shape. The 400–550-nm region of the spectra of both the L-His–$\alpha_2\beta_2$ and L-His–$\alpha_2\beta_2$–GP systems

[3] Although the description of an electronic transition as a log-normal distribution function is founded on some theoretical basis (though not in a strict absolute sense), the utility of the log-normal distribution curve lies in the accuracy with which these curves fit absorption bands (Siano & Metzler, 1969).

Table III: Summary of Parameters for the Simulation of Spectra in Figure 6 via the Summation of Log-Normal Distribution Curves

species	λ_{max}	absorbance at λ_{max}[a] $\alpha_2\beta_2$(L-His)$_2$	absorbance at λ_{max}[a] $(GP)_2\alpha_2\beta_2$-(L-His)$_2$	HW[b]	Ω[c]
$E(Q)_I$	469.5	0.135	0.55	1.2	1.1
$E(Q)_{II}$	444.6	0.046	0.18	1.4	1.4
E(Aex-K)	413.2	0.23	0.21	4.14	1.43

[a] Peak amplitude. [b] Peak width at half-height in units of 10^3 cm^{-1}. [c] Skewness of the curve [$\Omega = (V_v - V_0)/(V_0 - V_r)$, where V_0 is the wavenumber corresponding to λ_{max} and V_v and V_r are the wavenumber values at half-height on the "violet" and "red" sides of the curve, respectively].

are well described as the sum of three log-normal distribution curves (Figure 6 and Table III).[4] E(Q) is simulated by two log-normal distribution curves with a ratio of 3.0 ± 0.05 between the amplitudes of the two bands, designated in Table III as $E(Q)_I$ and $E(Q)_{II}$, observed both in the absence and in the presence of GP, respectively. The parameters for these curves are highly characteristic of the PLP quinonoid structure; there are two transitions with λ_{max} in the 450–550-nm range, an intense, narrow, longer wavelength transition and a weaker, broadened transition with a λ_{max} blue shifted approximately 1200 wavenumbers (27 nm). The ratio of the amplitudes of the two bands is typically between 3.3 and 1.5 (Kallen et al., 1985; Chen et al., 1987; D. E. Metzler, personal communication). The deviation of the simulated quinonoid band from the shape of the observed band in the vicinity of ~500 nm is typical and expected (Houben et al., 1989; Kallen et al., 1985; Metzler et al., 1973). E(Aex-K) is modeled by a single log-normal distribution curve with λ_{max} at ~413 nm. The log-normal parameters for this band (Table III) are characteristic of other ketoenamine tautomers (Metzler et al., 1980; Kallen et al., 1985). The lack of spectral dispersion and the abundance of possible chemical species that absorb in the 330-nm range preclude the fitting of this region with a unique set of log-normal distribution curves (Houben et al., 1989).

We conclude that the deconvoluted bands simulated by the log-normal distribution curves represent E(Aex-K) with λ_{max} 413.2 nm and E(Q) with λ_{max} 444.6 and 469.5 nm (see Scheme I), and as is evident in Table III, the position of the λ_{max}, the width at half-height (HW), the skewness (Ω) parameters, and the ratio of the amplitudes for the $E(Q)_I$ and $E(Q)_{II}$ bands are unaffected by the binding of GP. The log-normal fits shown in Figure 6 are not unique; alternative combinations of λ_{max}, bandwidth, and skewness for these bands can be found that give comparable fits. However, we have been unable to find another combination that gives the same amplitude ratio for the $E(Q)_I$ and $E(Q)_{II}$ bands both in the absence and in the presence of GP.

GP can be considered either an analogue of G3P (eqs 1 and 2) or an analogue of IGP (the α-subunit substrate for these reactions) (Yanofsky & Crawford, 1972; Heyn & Weischet, 1975; Miles, 1979). Evidence that GP and G3P bind to the same site on tryptophan synthase is indirect. The compound 3-indolepropanol 3′-phosphate (IPP) is an unreactive analogue of 3-indole-D-glycerol 3′-phosphate (IGP) that binds to the same site as IGP on the α-subunit (Kirschner et al., 1975a; Hyde et al., 1988). IGP and IPP induce circular dichroism signals that are very similar (Heyn & Weischet, 1975). Since IPP is competitive with respect to G3P (Weischet & Kirschner, 1976) and GP is competitive with respect to IPP (Heyn &

[4] The lower limit of 400 nm was chosen so that interference from the lower wavelength absorption bands would be minimized.

Weischet, 1975), it is very reasonable to presume that the effects of GP originate from binding interactions at the IGP catalytic site on the α-subunit. The distance between active sites of the α- and β-subunits is approximately 20–25 Å (Lane & Kirschner, 1983; Hyde et al., 1988). *Hence, long-range binding interactions involving distant loci on the protein bring about changes in the distribution of chemical intermediates along the catalytic pathway.* Consistent with the notion that these changes are mediated through long-range conformational changes is the finding that IPP also perturbs the spectrum of tryptophan synthase bound PLP intermediates formed with L-Trp (Kirschner et al., 1975b).

Changes in $\alpha_2\beta_2$ Affinity as a Result of Heterotropic Binding. Titration studies of either L-His or L-Trp with $\alpha_2\beta_2$ preequilibrated with saturating GP show that saturation of β-sites with amino acid is reached at a lower amino acid concentration. The apparent affinity for L-His increases approximately 4.5-fold ($K_{\text{L-His}}$ = 22 mM versus $K^{\text{GP}}_{\text{L-His}}$ = 4.8 mM; see Figure 2A and Table I), while the apparent affinity for L-Trp increases approximately 17-fold ($K_{\text{L-Trp}}$ = 0.35 mM versus $K^{\text{L-Trp}}_{\text{GP}}$ = 0.02 mM). These findings establish that GP also acts as a positive allosteric effector by stabilizing a form of the protein that has greater affinity for the amino acid quinonoid. The titrations give hyperbolic saturation curves indicating that the β-sites of the $\alpha_2\beta_2$ complex are identical, homogeneous, noncooperative sites (both in the presence and in the absence of GP) and that the subunit interactions mediated by GP binding are solely α–β interactions and not β–β.

Titration of the $\alpha_2\beta_2$(L-His)$_2$ complex with P_i (Figure 2B; Table I) yields a hyperbolic curve with $K^{\text{L-His}}_{\text{em}}$ = 46 mM_{em} (eq 4). The value of 46 $\text{mM}^{\text{L-His}}_{\text{em}}$ corresponds to a concentration of ~100 mM P_i (Robinson & Stokes, 1968). Hence, the concentration of 100 mM P_i buffer routinely used by workers in the tryptophan synthase field (Miles, 1979) corresponds to an effective concentration of P_i, which gives half of the absorbance change at 468 nm due to P_i in the $\alpha_2\beta_2$(L-His)$_2$ system. An early indication that P_i binds to the α-subunit catalytic site is the report that the IPP dissociation constant at pH 7.6 is 100 μM in phosphate buffer and 48 μM in Tris buffer (Kirschner & Wiskocil, 1972); as noted by Heyn and Weischet (1975), a K_I of 90 mM was calculated for P_i. The dissociation constants of the α-subunit for IPP and of the $\alpha_2\beta_2$ complex for IPP measured in 0.1 M phosphate buffer are both ~2.5-fold weaker than in Tris buffer (Kirschner et al., 1975b).

Kinetic Characterization of the DL-*α-Glycerol 3-Phosphate Mediated Allosteric Transition.* The RSSF and SWSF kinetic studies of the reaction of L-His with $\alpha_2\beta_2$ reveal the kinetic time course to consist of one detectable relaxation at low L-His concentrations (5–30 mM) and two relaxations at higher L-His concentrations (inset, Figure 3A). The small amplitude of the absorbance change at low concentrations of L-His precludes a definitive determination of the number of phases. Hence, either the single relaxation of 20 s^{-1} is a mean relaxation time consisting of two relaxation processes with the amplitude of one relaxation dominating the spectral changes, or the two relaxations at low L-His concentrations are too close together in rate to be resolved.

When L-His reacts with $\alpha_2\beta_2$ preequilibrated with saturating GP (Figure 3B), the spectral changes and relaxations are similar to that of the L-His reaction with $\alpha_2\beta_2$ in the absence of GP (Figure 3A), except that the amplitude changes are significantly larger. Again, at low L-His concentrations, a single relaxation (~20 s^{-1}) is sufficient to describe the time course; at high L-His concentrations at least two relaxations (~43 and ~15 s^{-1}) are required (inset, Figure 3B). The bimolecular linear mechanism eq 6 is the simplest system consistent with the data.

Equation 6 has been solved explicitly for the general case; however, the expressions for $1/\tau_1$ and $1/\tau_2$ are complex and ill-suited for the determination of the rate coefficients.[5] Given the nature of the experimental data, a unique solution of intrinsic rate constants for the L-His reaction with $\alpha_2\beta_2$ (in either the absence or presence of GP) cannot be obtained.

The relaxations observed in the mixing of GP with the $\alpha_2\beta_2$ complex preequilibrated with saturating L-His are consistent with the scheme shown in eq 7. The assignment of the 413-nm band to E(Aex-K) and the 445- and 469-nm bands to E(Q) together with the SWSF data and the previously discussed SWSF data for the reaction of L-His with $\alpha_2\beta_2$ are consistent with the expected chemical steps shown in eq 8 (viz. Scheme I). Equation 8 shows four chemical steps, implying four relaxations. The relaxation kinetic data give evidence for two unimolecular steps preceded by one bimolecular step. The presence of fewer relaxations than the four predicted indicates that either two of the relaxations are very similar in rate or the amplitude and/or rate of one relaxation is outside the detectability limits of the experimental method (Bernasconi, 1976).

$$\text{E} + \text{L-His} \rightleftharpoons \text{E(S)} \rightleftharpoons \text{T}_1 \rightleftharpoons \text{E(Aex-K)} \rightleftharpoons \text{E(Q)} \quad (8)$$

Since the barrier to conversion from E(S) to external aldimine is small in the L-Ser reaction with $\alpha_2\beta_2$ (Drewe & Dunn, 1985), and since E(S) formation is rapid, E(Aex-K) is the first intermediate to accumulate as a spectrophotometrically detectable species. The barrier to interconversion between the external aldimine tautomers [E(Aex-K) and E(Aex-E)] also should be very small (Scott et al., 1985). The reaction of $\alpha_2\beta_2$ with L-His behaves similarly; RSSF and SWSF data establish that the observed relaxations are tightly coupled, and both E(Aex-K) and E(Q) accumulate during $1/\tau_1$ and $1/\tau_2$. Therefore, only two observed relaxations are detected for the sequence of transformations depicted by Scheme I and eq 8.

P_i Heterotropic Effects. The observed rates when P_i is mixed with $\alpha_2\beta_2$ preequilibrated with saturating L-His are different from the rates observed in the analogous experiments involving GP. Since all steps are unimolecular and since the equilibrium constants $K_1 = k_1/k_{-1}$ and $K_2 = k_2/k_{-2}$ are not known independently, the intrinsic rate coefficients cannot be determined for either system (Bernasconi, 1976); nevertheless, because the observed relaxations (functions of the final intrinsic rate coefficients) are different for the GP and P_i systems, and because the changes in absorbance at 468 nm of the GP and P_i titrations extrapolated to infinite concentrations are different, GP and P_i must perturb the intrinsic rate coefficients to different extents.

When a solution containing both GP (20 mM) and P_i (163 mM_{em}) is mixed with $\alpha_2\beta_2$ preequilibrated with saturating L-His, the absorbance increase at 468 nm is biphasic (Figure 4, trace d) with relaxations of 28 and 8 s^{-1} (eq 5). Because the increase in absorbance is significantly greater than the sum of their separate effects [~0.35 AU vs ~0.25 AU (Figure 5)], the effects of both GP and P_i are synergistic. According to the titration data (see Figure 2B, isotherm a, and Table I), the concentration of GP used (20 mM) should be sufficient to saturate all of the IGP sites on the α-subunit. However,

[5] The general solution to eq 6 where the two steps equilibrate at similar rates gives $1/\tau_1 = (1/2)\sum k + [[(1/2)\sum k]2 - \prod k]^{1/2}$ and $1/\tau_2 = (1/2)\sum k - [[(1/2)\sum k]2 - \prod k]^{1/2}$, where $\sum k = k_1(C_A + C_B) + k_{-1} + k_2 + k_{-2}$, $\prod k = (k_1k_2 + k_1k_{-2})(C_A + C_B) + k_{-1}k_{-2}$, and C_A and C_B are the respective concentrations of species A and B (Bernasconi, 1976).

the best fit to eq 4 is not perfect, especially at the higher concentrations of GP.

Titration of the $\alpha_2\beta_2$ complex preequilibrated with saturating L-His (87 mM) and GP (24.2 mM) with P_i gives a single hyperbolic Langmuir isotherm (eq 4) with a best-fit $K_{em}^{L\text{-His,GP}} = 136\ mM_{em}$.[6] The absorbance increase at 468 nm estimated by extrapolating the isotherm to infinite $[P_i]$ gives a saturated value approximately 1.4-fold greater than the initial absorbance. Since the concentrations of both L-His and GP are essentially saturating (Figure 2), addition of P_i should not significantly increase the absorbance at 468 nm if P_i and GP bind only to the same site; hence, a second, synergistic phosphate interaction is strongly suggested. If the effects of GP and P_i are synergistic, then P_i interacts with $\alpha_2\beta_2$ at two loci, one distinct from the GP site. If this second site has physiological significance, then (because the affinity for P_i is so low) it is not a specific site for P_i but is likely a second site on $\alpha_2\beta_2$ designed for some other phosphorylated molecule.

Benzimidazole Heterotropic Effects. Kazarinoff and Snell (1980) have reported that the binding of indole induces a redistribution of bound intermediates formed in the reactions of L-Trp analogues with tryptophanase. Addition of benzimidazole (BZ) (an unreactive analogue of indole; Roy et al., 1988) to the tryptophan synthase $\alpha_2\beta_2$(L-Trp)$_2$ complex first increases and then decreases the amplitude of the L-Trp quinonoid 468-nm band (Lane & Kirschner, 1981). BZ exerts a similar effect on the amplitudes of the L-His quinonoid band in the presence of P_i (Figure 5B,a). In the absence of P_i, BZ only decreases the amplitude of the quinonoid absorption band (Figure 5B,b). The biphasic equilibrium data of Figure 5B,a can be explained by the following argument: Since the interaction of P_i generates a high-affinity site for the indole moiety of IGP (Weischet & Kirschner, 1976), the increase in absorbance at 468 nm is due to BZ binding to the indole subsite of the α-catalytic center.[7] This binding confers additional interactions that drive the $\alpha_2\beta_2$ complex to a conformation which stabilizes quinonoid species. At higher concentrations, competition between BZ and the imidazolyl moiety of L-His for the indole subsite of the β-catalytic site becomes significant and the L-His quinonoid is displaced. In the absence of P_i, no high-affinity indole-like subsite on the α-subunit is generated and only the displacement of L-Trp or L-His by BZ from the β-catalytic site takes place, thereby resulting only in a decrease in absorbance at 468 nm. Indole has a greater affinity for the β-catalytic site than for the α-catalytic site when the β PLP site is ligated. If indole (the natural substrate) were bound more tightly at the α-catalytic site than at the β-site, L-Trp production would be inhibited. Thus, in the absence or presence of P_i, indole only produces a decrease in the L-His or L-Trp quinonoid species (data not shown).

Mechanistic Implications of the Allosteric Interactions. These studies establish that noncovalent binding of ligands such as GP or P_i to the α-subunit brings about a redistribution of the bound covalent intermediates formed in the reactions of amino acids with the β-subunits of $\alpha_2\beta_2$. We conclude that these redistributions occur via the alteration of the relative ground-state free energies of the bound intermediates. Since the rate constants for interconversion in the tryptophan synthase system are changed, the free energies of the activated complexes for the interconversion of these intermediates must also be changed. The GP-induced redistribution of intermediates at the β-site favors the quinonoid structure [E(Q) in Scheme I], giving roughly a 4-fold increase in the amount of quinonoid species (compare panels A and B of Figure 6).

We postulate that the redistribution of chemical intermediates occurs as follows: (1) As substrate undergoes transformation from one intermediate to the next, the enzyme site undergoes obligatory conformational changes to accommodate and assist structural and electronic changes in the reacting substrate. (2) In the tryptophan synthase system, substrates participate both as reactants and as noncovalent effectors in driving the protein conformation changes which are obligatory for the conversion of one intermediate to the next. (3) Consequently, weak bonding interactions between protein and effector (exemplified by GP) are used to lower the activation energies for the interconversion of intermediates (and protein conformations). (4) The redistribution of bound intermediates brought about by effectors and/or substrates or substrate analogues is the consequence of preferential binding to a particular enzyme conformation that lies along the reaction path.

The affinity of $\alpha_2\beta_2$ for L-His or L-Trp increases as a result of GP binding to the α-site (Tables I and II). If L-His (or L-Trp) and GP mimic the actions of the physiological substrates L-Ser and IGP, then the reciprocal increase in affinities of $\alpha_2\beta_2$ for L-His (or L-Trp) and GP when both are bound is significant. As proposed in the preceding paragraph, it is likely that substrates participate both as reactants and as effectors in the $\alpha_2\beta_2$ system, but the effector role in this case not only drives obligatory protein conformational changes for the conversion of one intermediate to the next but also modulates the affinity of protein for cosubstrate so that the transfer of indole from the α-site to the β-site is favored and the probability of conversion of substrates to product is increased. In this regard, it is worthwhile to examine the role of ligands in tryptophan synthase catalysis, especially with respect to the analogues GP and IPP, which on occasion have been labeled inhibitory because the two ligands apparently decrease the turnover rate of reaction (eq 3) (Kawasaki et al., 1987; Lane & Kirschner, 1981). The influence of an alleged effector molecule can depend on the concentration of the substrate; for example, if the effector molecule increases the affinity of the enzyme for the substrate but reduces the rate of catalysis, then the effector molecule may function as an activator at low substrate concentrations and as an inhibitor at high substrate concentrations. For L-Trp formation, it is advantageous for the system if L-Ser interacts less strongly with β-sites that cannot carry out the aldol-like condensation reaction with indole (due to the absence of IGP at the α-subunit site). The GP and BZ binding studies presented herein predict that when IGP is present (cleaved or intact) on the α-subunit, the β-site becomes a higher affinity site for L-Ser and the chemical transformations are driven in favor of C–C bond synthesis

[6] If the concentration of GP is less than that required to saturate the α-catalytic sites when the β PLP site is titrated with a particular ligand, then titration of that ligand to the β-site will produce data that will not fit a single hyperbolic isotherm. Because two different α_2b_2–ligand complexes are present, one with GP bound and the other without, the two enzyme forms have different affinities for the β ligand and likely have different distributions of β-bound intermediates analogous to the L-Trp or L-His systems in the absence and presence of GP. When P_i is substituted for GP in the above-described titration experiments, the same arguments hold. Hence, data from titrations performed in 0.1 M phosphate buffer deviate from a single hyperbolic isotherm.

[7] Additional evidence (Houben, 1988) for this notion is that indole at concentrations above 0.2 mM inhibits the reaction (eq 3) when P_i is present (Kirschner et al., 1975a,b; Lane & Kirschner, 1983). Since IPP or GP binding to the α-subunit inhibits this reaction (Lane & Kirschner, 1981; Kawasaki et al., 1987), inhibition by indole with P_i present probably occurs through indole binding to the α-subunit indole subsite generated by P_i binding.

between indole and the α-aminoacrylate Schiff base intermediate, thereby increasing the probability of L-Trp synthesis.

References

Adachi, O., Kohn, L. D., & Miles, E. W. (1974) *J. Biol. Chem. 249*, 7756–7763.

Bernasconi, C. F. (1976) in *Relaxation Kinetics*, pp 13, Academic Press, New York.

Chen, V. J., Metzler, D. E., & Jenkins, W. T. (1987) *J. Biol. Chem. 262*, 14422–14427.

Drewe, W. F., Jr., & Dunn, M. F. (1985) *Biochemistry 24*, 3977–3987.

Drewe, W. F., Jr., & Dunn, M. F. (1986) *Biochemistry 25*, 2494–2501.

Drewe, W. F., Jr., Koerber, S. C., & Dunn, M. F. (1989) *Biochimie 71*, 509–519.

Dunn, M. F., Roy, M., Robustell, B., & Aguilar, V. (1987) in *Proceedings of the 1987 International Congress on Chemical and Biological Aspects of Vitamin B_6 Catalysis* (Korpela, T., & Christen, P., Eds.) pp 171–181, Birkhäuser, Basel.

Heyn, M. P., & Weischet, W. O. (1975) *Biochemistry 14*, 2962–2968.

Houben, K. F. (1988) Dissertation, University of California, Riverside.

Houben, K. F., Kadima, W., Roy, M., & Dunn, M. F. (1989) *Biochemistry 28*, 4140–4147.

Hyde, C. C., Padlan, E. A., Ahmed, S. A., Miles, E. W., & Davies, D. R. (1988) *J. Biol. Chem. 263*, 17857–17871.

Kallen, R. G., Korpela, T., Martell, A. E., Matsushima, Y., Metzler, C. M., Metzler, D. E., Morozov, Y. V., Ralston, I. M., Savin, F. A., Torchinsky, Y. M., & Ueno, H. (1985) in *Transaminases* (Christen, P., & Metzler, D., Eds.) pp 37–109, Wiley and Sons, New York.

Kawasaki, H., Baurle, R., Zon, G., Ahmed, S. A., & Miles, E. S. (1987) *J. Biol. Chem. 262*, 10678–10683.

Kazarinoff, M. N., & Snell, E. E. (1980) *J. Biol. Chem. 255*, 6228–6235.

Kirschner, K., & Wiskocil, R. L. (1972) in *Protein–Protein Interactions* (Jaenicke, R., & Helmreich, E., Eds.) pp 245–269, Springer-Verlag, Heidelberg.

Kirschner, K., Weischet, W., & Wiskocil, R. L. (1975a) in *Protein–Ligand Interactions* (Sund, H., & Blaver, G., Eds.) pp 27–44, de Gruyter, Berlin.

Kirschner, K., Wiskocil, R. L., Foehn, M., & Rezeau, L. (1975b) *Eur. J. Biochem. 60*, 513–523.

Koshland, D. E., Nemethy, G., & Filmer, D. (1966) *Biochemistry 5*, 365–385.

Lane, A. N., & Kirschner, K. (1981) *Eur. J. Biochem. 120*, 379–387.

Lane, A. N., & Kirschner, K. (1983) *Eur. J. Biochem. 129*, 675–684.

Likos, J. L., Ueno, H., Feldhaus, R. W., & Metzler, D. E. (1982) *Biochemistry 21*, 4377–4386.

Matchett, W. H. (1974) *J. Biol. Chem. 249*, 4041–4049.

Metzler, C. M., Cahill, A. E., & Metzler, D. E. (1980) *J. Am. Chem. Soc. 102*, 6075–6082.

Metzler, C. M., Cahill, A. E., Petty, S., Metzler, D. E., & Lang, L. (1985) *Appl. Spectrosc. 39*, 333–339.

Metzler, D. E., Harris, C. M., Johnson, R. J., Siano, D. B., & Thomson, J. A. (1973) *Biochemistry 12*, 5377–5392.

Miles, E. W. (1979) *Adv. Enzymol. 49*, 127–186.

Miles, E. W., & Moriguchi, M. (1977) *J. Biol. Chem. 252*, 6594–6599.

Monod, J., Wyman, J., & Changeux, J.-P. (1965) *J. Mol. Biol. 12*, 88–118.

Moore, J. W., & Pearson, R. G. (1981) in *Kinetics and Mechanism*, 3rd ed., pp 284–329, Wiley, Canada.

Robinson, R. A., & Stokes, R. H. (1968) in *Electrolyte Solutions*, 2nd ed., Butterworth, London.

Roy, M., Kieblawi, S., & Dunn, M. F. (1988) *Biochemistry 27*, 6698–6704.

Scott, R. D., Chang, Y.-C., Graves, D. J., & Metzler, D. E. (1985) *Biochemistry 24*, 7668–7681.

Siano, D. B., & Metzler, D. E. (1969) *J. Chem. Phys. 51*, 1856–1861.

Srivastava, D. K., & Bernhard, S. A. (1986a) *Science 234*, 1081–1086.

Srivastava, D. K., & Bernhard, S. A. (1986b) *Curr. Top. Cell. Regul. 28*, 1–68.

Tschopp, J., & Kirschner, K. (1980) *Biochemistry 19*, 4514–4521, 4251–4527.

Weischet, W. O., & Kirschner, K. (1976) *Eur. J. Biochem. 65*, 365–373.

Wilhelm, P., Pilz, I., Lane, A. N., & Kirschner, K. (1982) *Eur. J. Biochem. 129*, 51–56.

Yanofsky, C., & Crawford, I. P. (1972) *Enzymes (3rd Ed.) 8*, 1–31.